

## Supporting Information

### **Plasma Ag nanoparticles loaded on Bi<sub>2</sub>MoO<sub>6</sub> to enhance surface oxygen vacancies for efficient nitrogen conversion to ammonia**

Zhenyu Liu, Min Luo\*, Linghu Meng, Senda Su, Wenming Ding, Shengbo Yuan, Hua Li, Xiaoman Li\*

State Key Laboratory of High-efficiency Utilization of Coal and Green Chemical Engineering, School of Chemistry and Chemical Engineering, Ningxia University, Yinchuan, Ningxia 750021, China

E-mail: [luominjy@nxu.edu.cn](mailto:luominjy@nxu.edu.cn), [lixm2017@nxu.edu.cn](mailto:lixm2017@nxu.edu.cn).

# CONTENT

1. **S1.** Materials.
2. **S2.** Characterizations.
3. **S3.** The synthesis of BMO and Ag/BMO.
4. **S4.** Visible-light photocatalytic nitrogen fixation experiments.
5. **S5.** Photoelectrochemical Measurements.
6. **Fig. S1.** (a) The UV-Vis absorption spectra of  $\text{NH}_4^+$  determined by Nessler's reagent. (b) The standard curves used to calculate the  $\text{NH}_4^+$  concentration.
7. **Fig. S2.** Nitrogen adsorption-desorption isotherms of pure phase BMO and 1% Ag/BMO.
8. **Fig. S3.** LSV curve of 1% Ag/BMO in dark and under light irradiation.
9. **Fig. S4.** The relationship between the mass of 1% Ag/BMO photocatalyst and photocatalytic nitrogen fixation activity.
10. **Fig. S5.** The SEM image of 1% Ag/BMO after irradiation.
11. **Fig. S6.** XRD patterns of 1% Ag/BMO before and after irradiation.
12. **Fig. S7.** XPS spectra of 1% Ag/BMO after irradiation: (a) survey, (b) Bi 4f, (c) Mo 3d, (d) O 1s, and (e) Ag 3d.
13. **Fig. S8.** (a) Standard curve of measurement of ammonia by IC; (b) Determination of  $\text{NH}_4^+$  concentration of 1% Ag/BMO after photocatalyzed for 1h by IC.
14. **Fig. S9.** The Water contact angles of BMO (a) and 1% Ag/BMO (b).
15. **Table S1.** Real contents of Ag in the 1% Ag/BMO, 5% Ag/BMO, and 10% Ag/BMO with the measurement of ICP-OES.
16. **Table S2.** The datas were obtained by fitting the time-resolved PL decay curves to a tri-exponential model.
17. **Table S3.** Photocatalytic nitrogen fixation performance of different photocatalysts.

## S1. Materials.

For the entire experiment, all chemicals used were analytical grade without purification and ultrapure water was acquired from a Milli-Q system (resistivity  $\geq 18.2 \text{ M}\Omega \text{ cm}$ ). Bismuthnitrate pentahydrate ( $\text{Bi}(\text{NO}_3)_3 \cdot 5\text{H}_2\text{O}$ ), sodium molybdate dihydrate ( $\text{Na}_2\text{MoO}_4 \cdot 2\text{H}_2\text{O}$ ), and ethylene glycol ( $\text{C}_2\text{H}_6\text{O}_2$ ) were provided by Macklin Biochemical Technology Co., Ltd. (Shanghai, China). Silver nitrate ( $\text{AgNO}_3$ ) and anhydrous ethanol ( $\text{C}_2\text{H}_5\text{OH}$ ) were provided by Sinopharm Chemical Reagent Co., Ltd. (Shanghai, China).

## S2. Characterizations.

The crystalline phase structure of the samples was obtained by X-ray powder diffractometer (XRD, Bruker, D8 Advance, Germany) over a scanning range of  $3\text{-}80^\circ$  at a rate of  $2^\circ/\text{min}$ . The surface morphology of the samples was taken by scanning electron microscopy (SEM, ZEISS, Sigma 300, Germany). The morphology and elemental distribution of the samples could also be acquired by a transmission electron microscope (TEM, JEOL, JEM-F200, Japan) equipped with an energy dispersive X-ray spectrometer (EDS). The elemental surface composition and valence band information of the samples were acquired under high vacuum conditions on X-ray photoelectron spectroscopy (XPS, Thermo Scientific, ESCALAB Xi+, USA). The contact angles were tested using a surface tension meter (Kunshan Shengding, SDC 350KS, China). The data of UV-vis diffuse reflectance spectra (UV-vis DRS) and absorbance were known from a UV-vis spectrophotometer using  $\text{BaSO}_4$  as a reference whiteboard (PERSEE, TU-1901, China). The fluorescence properties including photoluminescence spectra (PL) and time-resolved photoluminescence (TRPL) spectra were performed by a steady-state/transient fluorescence spectrometer (Edinburgh, FLS1000, UK). The quantitative analysis of the element of the materials were carried out by inductively coupled plasma optical emission spectroscopy (ICP-OES, Agilent, ICPOES730, USA). The visible light source was provided by a xenon lamp (Perfect, PLS-SXE 300, China). Electron paramagnetic resonance (EPR) spectra were carried out the (Bruker, EMXplus-6/1, Germany) paramagnetic resonance

spectrometer. Nitrogen temperature-programmed desorption ( $N_2$ -TPD, Micromeritics, AutoChem II 2920, USA) was conducted in a quartz reactor with a TCD detector. Ion chromatography (IC, Dionex AQUION RFIC, Thermo scientific, Mexico) obtained on an ion chromatograph.

**S3.** The synthesis of BMO and Ag/BMO.

### **The synthesis of BMO**

To begin with, 2 mmol  $Bi(NO_3)_3 \cdot 5H_2O$  and 1 mmol  $Na_2MoO_4 \cdot 2H_2O$  were each ultrasonically dissolved within 10 mL of ethylene glycol and mixed well. Then, in constant stirring, a colorless and transparent solution was formed by slowly dropping the above mixed solution into 40 mL of ethanol. The resultant mixed solution was transferred to a 100 mL Teflon-lined stainless steel autoclave and solvothermal treatment was carried out over 24 h at 160 °C. Finally, the yellow precipitate was separated by centrifugation and the precipitate was washed multiple times with ultrapure water and ethanol, respectively, and dried, and the BMO sample was obtained after the above steps.

### **The synthesis of Ag/BMO**

The synthesized steps of Ag/BMO were as follows: Firstly, 100 mg of BMO sample was placed in 60 mL of ethylene glycol and dispersed uniformly by ultrasonic treatment. Next, a certain amount of  $AgNO_3$  solid was added and kept stirring for 1 h under the condition of avoiding light. Here, the mass of  $AgNO_3$  referred to the molar ratios of  $AgNO_3$  to BMO of 0%, 0.5%, 1 %, 5 %, and 10 %, respectively. Then, the resulting suspension was transferred to a 100 mL Teflon-lined stainless steel autoclave and solvothermal treatment was carried out over 24 h at 160 °C. Finally, the precipitate was separated by centrifugation, this precipitate was washed multiple times with ultrapure water and ethanol, respectively, and dried to obtain the final Ag/BMO sample. The samples were recorded as BMO-2, 0.5% Ag/BMO, 1% Ag/BMO, 5% Ag/BMO, and 10% Ag/BMO, respectively.

**S4.** Visible-light photocatalytic nitrogen fixation experiments.

The photocatalytic nitrogen fixation reaction was carried out at room temperature

in a closed reactor equipped with a cooling water circulation system. The top of the reactor was fixed with a 300 W xenon lamp equipped with a cut-off filter at 420 nm. The procedure was as follows: First, 30 mg of photocatalyst and 100 mL of ultrapure water were placed in a reactor and ultrasonically dispersed into a uniform suspension. Next, high-purity N<sub>2</sub> was passed into the suspension at a flow rate of 80 mL min<sup>-1</sup> and stirred in the dark for 30 min to achieve adsorption-desorption equilibrium. Subsequently, the xenon lamp was switched on to start the reaction with the suspension collected at 30 min intervals and centrifuged to obtain the supernatant. Finally, the ammonia content in the solution was determined by monitoring its absorbance at 420 nm with a UV-vis spectrophotometer using Nessler's reagent method. The concentration of NH<sub>4</sub><sup>+</sup> was determined from standard curves plotted using different concentrations of standard NH<sub>4</sub><sup>+</sup> solutions, as shown in Fig. S1.

#### **S5. Photoelectrochemical Measurements.**

The photoelectrochemical properties of the photocatalysts were carried out at an electrochemical workstation (CH Instruments, CHI-760E, China) equipped with a standard three-electrode system and 0.1 M Na<sub>2</sub>SO<sub>4</sub> electrolyte. The standard three-electrode system consists of a platinum sheet counter electrode, a saturated Ag/AgCl reference electrode and a working electrode. The method of making the working electrode was as follows: 4 mg of photocatalyst was dispersed in 0.4 mL of ethanol and 8 μL of Nafion reagent (5 wt%) to form a uniform dispersion. Then, it was spin-coated onto pretreated indium tin oxide (ITO) glass and dried naturally overnight.

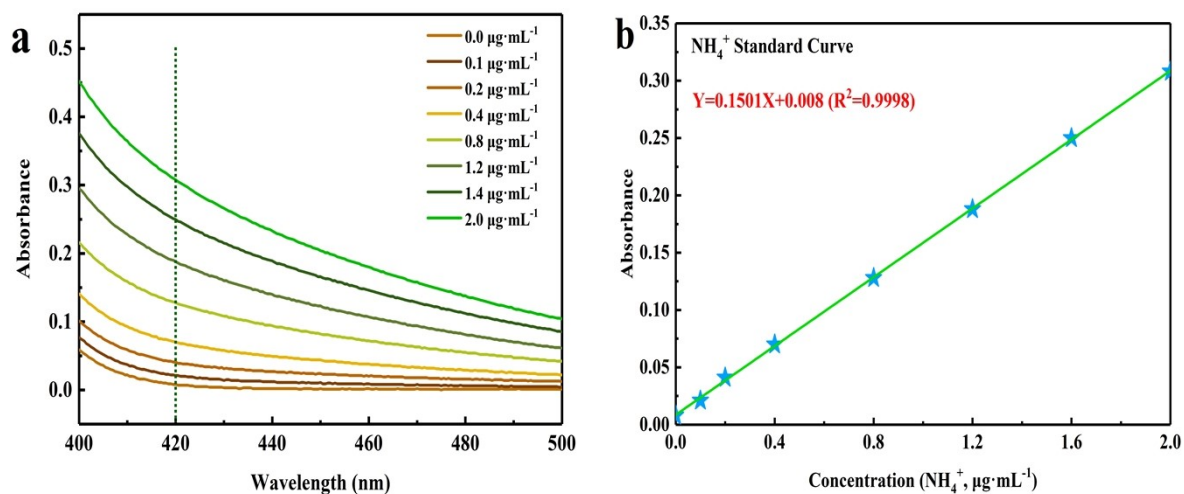


**Fig. S1.** (a) The UV-Vis absorption spectra of  $\text{NH}_4^+$  determined by Nessler's reagent. (b) The standard curves used to calculate the  $\text{NH}_4^+$  concentration.

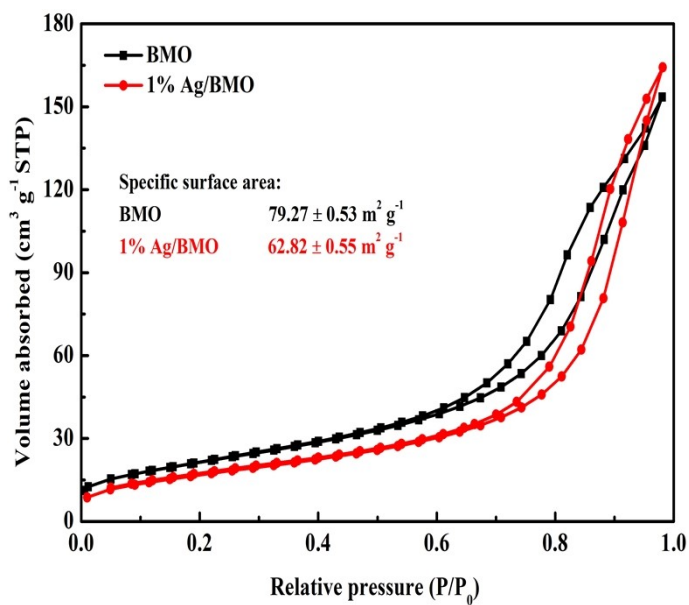


**Fig. S2.** Nitrogen adsorption-desorption isotherms of pure phase BMO and 1% Ag/BMO.

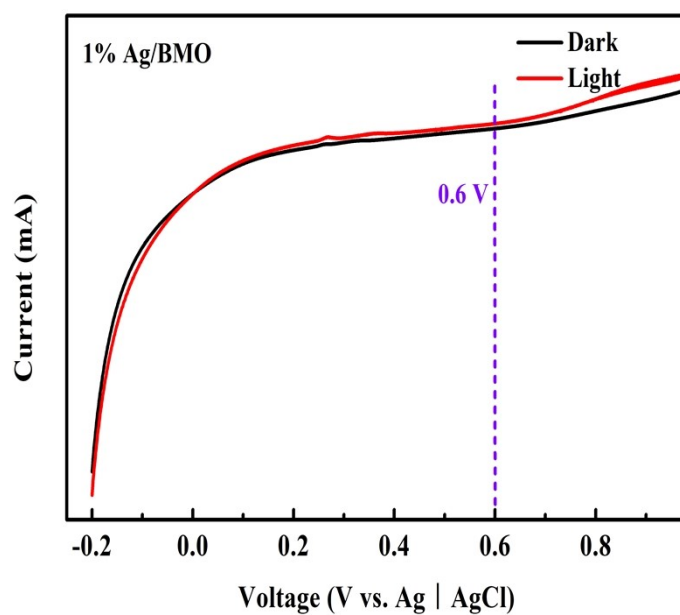


**Fig. S3.** LSV curve of 1% Ag/BMO in dark and under light irradiation.

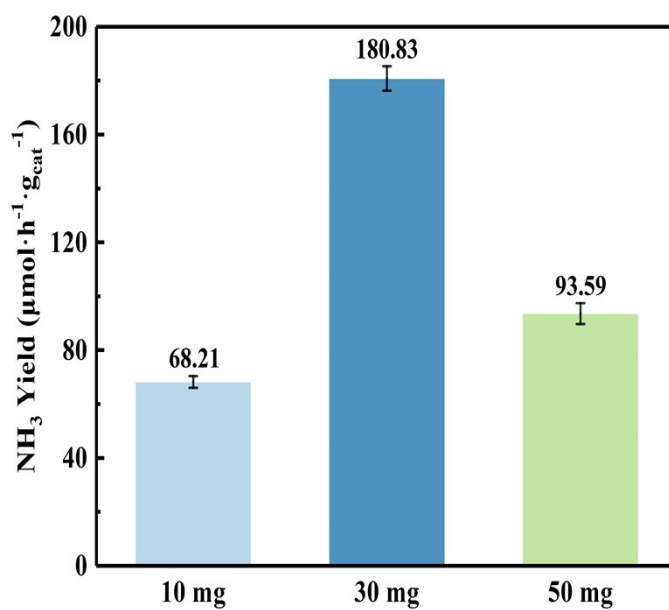


**Fig. S4.** The relationship between the mass of 1% Ag/BMO photocatalyst and photocatalytic nitrogen fixation activity.

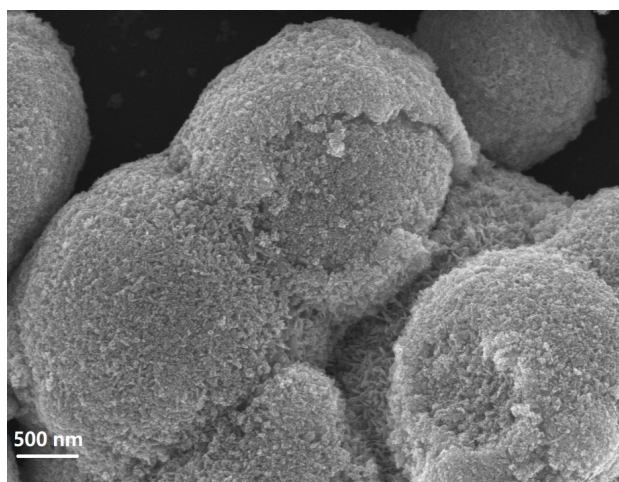


**Fig. S5.** The SEM image of 1% Ag/BMO after irradiation.

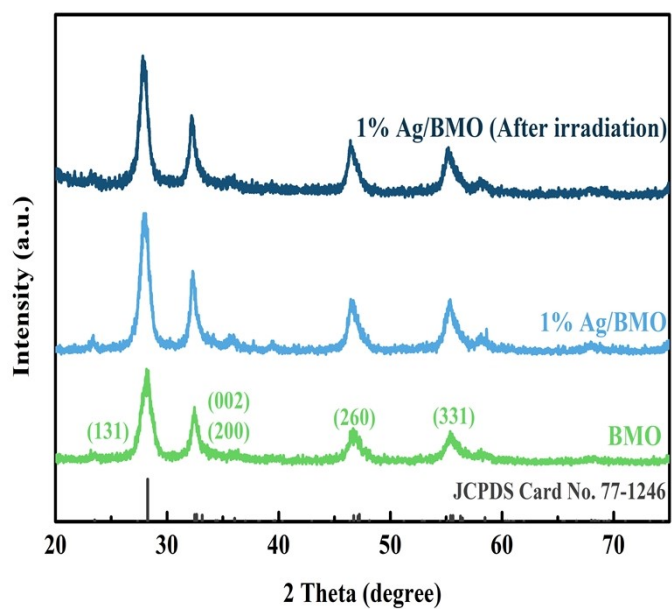


**Fig. S6.** XRD patterns of 1% Ag/BMO before and after irradiation.



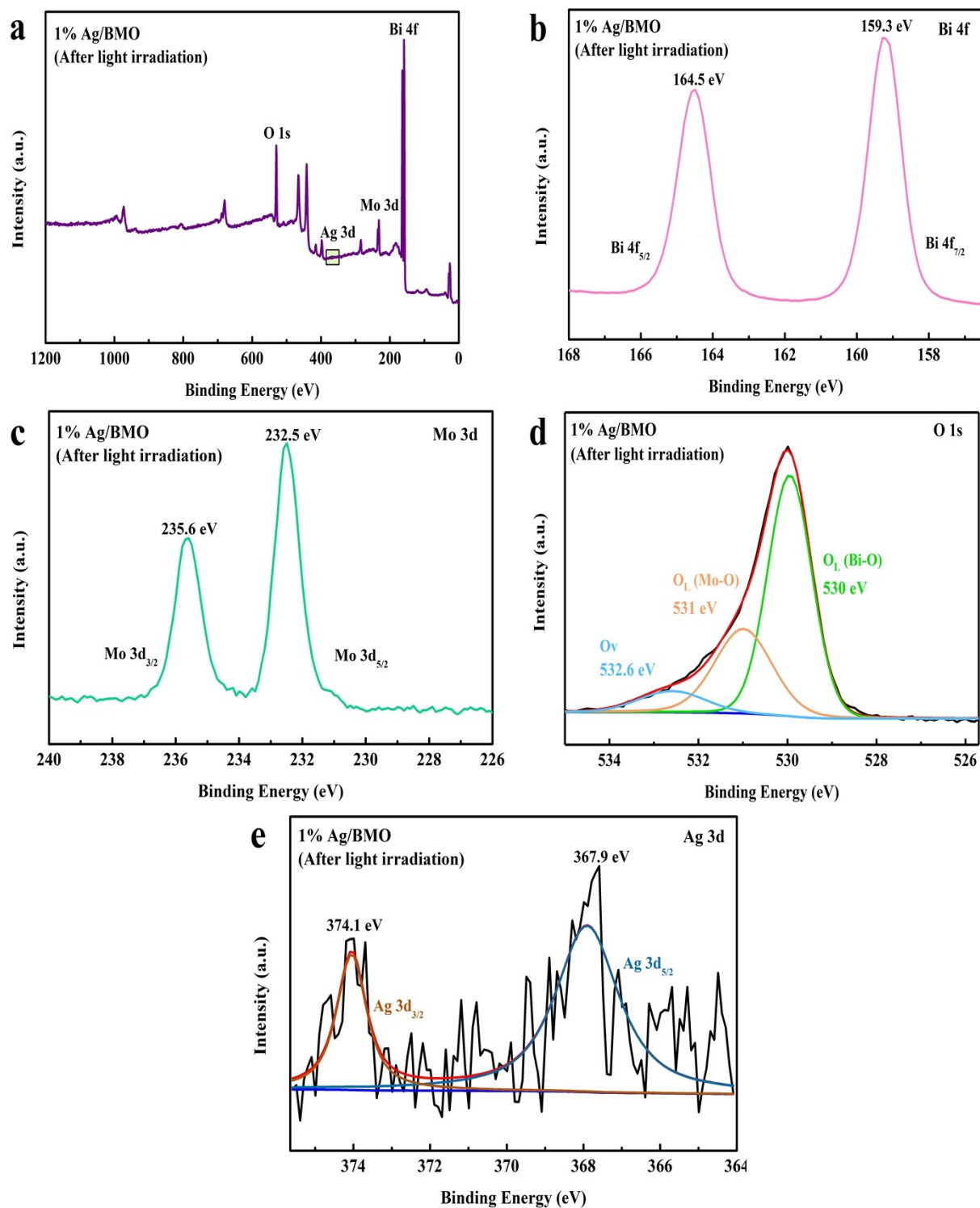


**Fig. S7.** XPS spectra of 1% Ag/BMO after irradiation: (a) survey, (b) Bi 4f, (c) Mo 3d, (d) O 1s, and (e) Ag 3d.

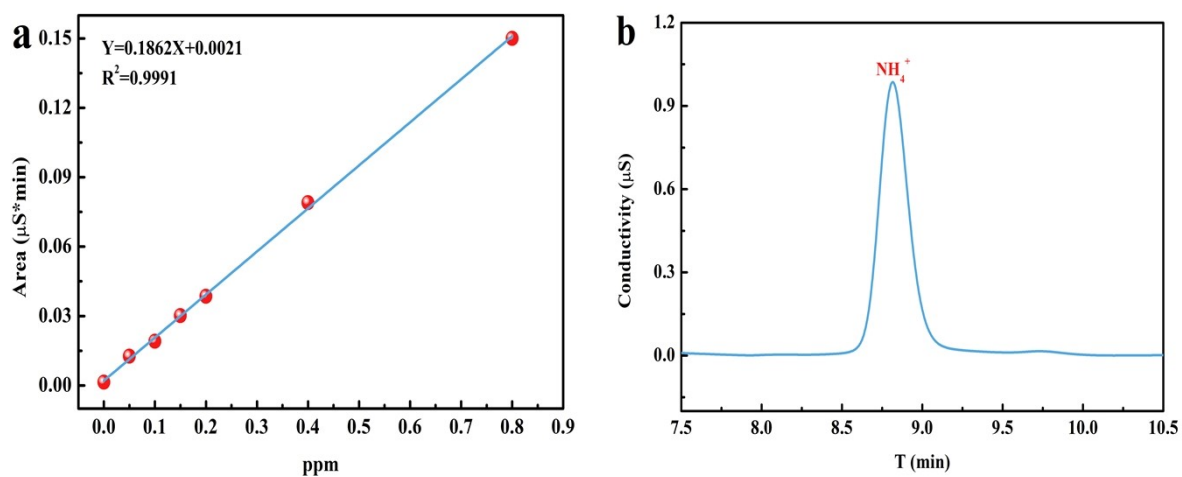


**Fig. S8.** (a) Standard curve of measurement of ammonia by IC; (b) Determination of NH<sub>4</sub><sup>+</sup> concentration of 1% Ag/BMO after photocatalyzed for 1h by IC.

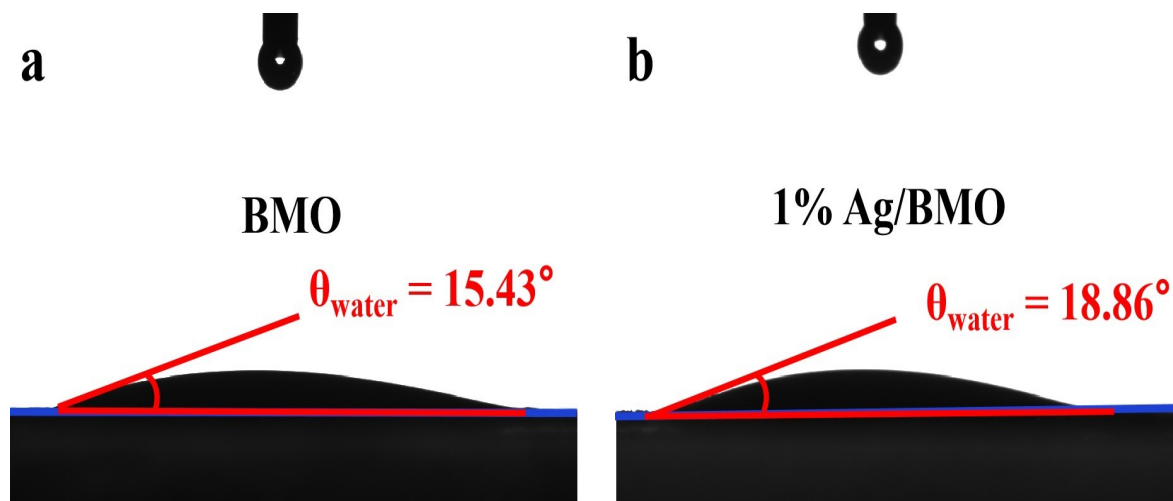


**Fig. S9.** The Water contact angles of BMO (a) and 1% Ag/BMO (b).

**Table S1.** Real contents of Ag in the 0.5% Ag/BMO, 1% Ag/BMO, 5% Ag/BMO, and 10% Ag/BMO with the measurement of ICP-MS.

<b>Samples</b>	<b>Theoretical AgNO<sub>3</sub>/BMO (Molar ratio, %)</b>	<b>Theoretical Ag element content (Wt. %)</b>	<b>Real element content of Ag (Wt. %)</b>
<b>0.5% Ag/BMO</b>	0.5	0.14	0.11
<b>1% Ag/BMO</b>	1	0.28	0.24
<b>5% Ag/BMO</b>	5	1.4	1.1
<b>10% Ag/BMO</b>	10	2.8	2.6

**Table S2.** The datas were obtained by fitting the time-resolved PL decay curves to a tri-exponential model.

<b>Samples</b>	<b><math>\tau_1</math> (ns)</b>	<b><math>\tau_2</math> (ns)</b>	<b><math>\tau_3</math> (ns)</b>	<b>B<sub>1</sub> (%)</b>	<b>B<sub>2</sub> (%)</b>	<b>B<sub>3</sub> (%)</b>	<b><math>\tau_{avg}</math> (ns)</b>
<b>BMO</b>	0.78	3.89	47.04	13.23	17.54	69.22	33.35
<b>1% Ag@BMO</b>	0.77	3.31	29.40	35.63	26.86	37.51	12.19

**Table S3.** Photocatalytic nitrogen fixation performance of different photocatalysts.

Photocatalysts	Light source	organic scavenger	NH <sub>3</sub> generation rate ( $\mu\text{mol g}^{-1} \text{h}^{-1}$ ) <sup>1)</sup>	Reference
<b>2.5% Ag/Bi<sub>5</sub>O<sub>7</sub>I</b>	300 W Xe lamp, Full spectrum	None	40.2	[1]
		Isopropanol	40.2	
		C <sub>2</sub> H <sub>5</sub> OH	81.4	
<b>Cu-g-C<sub>3</sub>N<sub>4</sub></b>	300 W Xe lamp, $\lambda > 420 \text{ nm}$	CH <sub>3</sub> OH	178.2	[2]
		C <sub>2</sub> H <sub>5</sub> OH	186	
<b>Pt/O-NaNbO<sub>3</sub></b>	300 W Xe lamp, Full spectrum	CH <sub>3</sub> OH	293	[3]
<b>PtBi/KTa<sub>0.5</sub>Nb<sub>0.5</sub>O<sub>3</sub></b>	300 W Xe lamp, Full spectrum	CH <sub>3</sub> OH	385	[4]
<b>Bi-Bi<sub>2</sub>O<sub>3</sub>/KTa<sub>0.5</sub>Nb<sub>0.5</sub>O<sub>3</sub></b>	300 W Xe lamp, Full spectrum	CH <sub>3</sub> OH	466	[5]
<b>Pt/CdMoO<sub>4</sub></b>	300 W Xe lamp, Full spectrum	CH <sub>3</sub> OH	443.7	[6]
<b>1% Ag/BMO</b>	300 W Xe lamp, $\lambda > 420 \text{ nm}$	None	247.45	<b>This work</b>

## References

- [1] Chen, L., Zhang, W. Q., Wang, J. F., Li, X. J., Li, Y., Hu, X., Zhao, L. H., Wu, Y., He, Y. M., High piezo/photocatalytic efficiency of Ag/Bi<sub>5</sub>O<sub>7</sub>I nanocomposite using mechanical and solar energy for N<sub>2</sub> fixation and methyl orange degradation, *Green Energy Environ.* 8 (1) (2023) 283-295. <https://doi.org/10.1016/j.gee.2021.04.009>.
- [2] Huang, P. C., Liu, W., He, Z. H., Xiao, C., Yao, T., Zou, Y. M., Wang, C. M., Qi, Tong, W., Pan, B. C., Wei, S. Q., Xie, Y., Single atom accelerates ammonia photosynthesis, *Science*

China Chemistry. 61 (2018) 1187-1196. <https://doi.org/10.1007/s11426-018-9273-1>.

- [3] Zhang J, Yue L, Zeng Z, et al. Preparation of  $\text{NaNbO}_3$  microcube with abundant oxygen vacancies and its high photocatalytic  $\text{N}_2$  fixation activity in the help of Pt nanoparticles[J]. Journal of Colloid and Interface Science, 2023, 636: 480-491.
- [4] Li, X. J., Chen, L., Wang, J. F., Zhang, J. Y., Zhao, C. R., Lin, H. J., Wu, Y., He, Y. M., Novel platinum-bismuth alloy loaded  $\text{KTa}_{0.5}\text{Nb}_{0.5}\text{O}_3$  composite photocatalyst for effective nitrogen-to-ammonium conversion, J. Colloid. Interf. Sci. 618 (2022) 362-374. <https://doi.org/10.1016/j.jcis.2022.03.096>.
- [5] Chen, L., Wang, J. F., Li, X. J., Zhao, C. R., Hu, X., Wu, Y., He, Y. M., A novel Z-scheme  $\text{Bi}_2\text{O}_3/\text{KTa}_{0.5}\text{Nb}_{0.5}\text{O}_3$  heterojunction for efficient photocatalytic conversion of  $\text{N}_2$  to  $\text{NH}_3$ , Inorg. Chem. Front. 9 (11) (2022) 2714-2724. <https://doi.org/10.1039/D2QI00175F>.
- [6] Ren, X. J., Wang, J. F., Yuan, S. D., Zhao, C. R., Yue, L., Zeng, Z. H., He, Y. M., Decoration of  $\text{CdMoO}_4$  micron polyhedron with Pt nanoparticle and their enhanced photocatalytic performance in  $\text{N}_2$  fixation and water purification, Front. Chem. Sci. Eng. 17 (12) (2023) 1949-1961. <https://doi.org/10.1007/s11705-023-2360-6>.